Supplement of Atmos. Meas. Tech., 19, 5753–5783, 2026
https://doi.org/10.5194/amt-19-5753-2026-supplement

Atmospheric Measurement Techniques
Open Access
EGU

Supplement of

Characterization of Saharan and Middle Eastern dust aerosols and their associated shortwave direct radiative effects over Cyprus

Georgia Charalampous et al.

Correspondence to: Georgia Charalampous (georgia.charalambous@eratosthenes.org.cy)

Supplementary Tables

Table S1: Seasonal meteorological conditions at the Xyliatos Dam meteorological station during September 2015–December 2022. Values represent the mean ± standard deviation of daily mean air temperature, daily mean relative humidity and daily mean wind speed.

Season	Days	Air temperature (°C)	Relative humidity (%)	Mean wind speed (m s^{-1})	Prevailing wind sector	Sector frequency (%)
DJF	654	10.1 ± 3.0	67.0 ± 10.6	1.07 ± 0.51	S	28.0
MAM	634	16.9 ± 5.6	49.7 ± 16.8	1.36 ± 0.52	S	19.4
JJA	644	26.9 ± 3.0	43.9 ± 15.3	1.49 ± 0.27	NNW	26.4
SON	724	20.2 ± 4.5	54.9 ± 14.8	1.16 ± 0.31	S	27.2

Table S2: Statistical summary of the AERONET-Dubovik aerosol classification for the Agia Marina Xyliatou (AMX) station during 2015–2022. Statistics are calculated using all individual AERONET observations included in the aerosol classification.

Aerosol Type	N	AOD_{440} (Mean ± SD)	AOD_{440} Median [Q1–Q3]	$AE_{440–870}$ (Mean ± SD)	$AE_{440–870}$ Median [Q1–Q3]
Marine	10,632	0.11 ± 0.05	0.11 [0.07–0.15]	0.87 ± 0.27	0.94 [0.69–1.09]
Biomass burning / polluted	1,803	0.28 ± 0.08	0.25 [0.22–0.29]	1.71 ± 0.08	1.70 [1.65–1.75]
Dust	3,499	0.30 ± 0.11	0.27 [0.23–0.33]	0.48 ± 0.27	0.42 [0.26–0.71]
Mixed	3,591	0.28 ± 0.08	0.26 [0.23–0.31]	1.37 ± 0.17	1.41 [1.24–1.51]
Continental	15,721	0.11 ± 0.04	0.11 [0.08–0.15]	1.50 ± 0.20	1.48 [1.35–1.63]

Supplement Additional figures

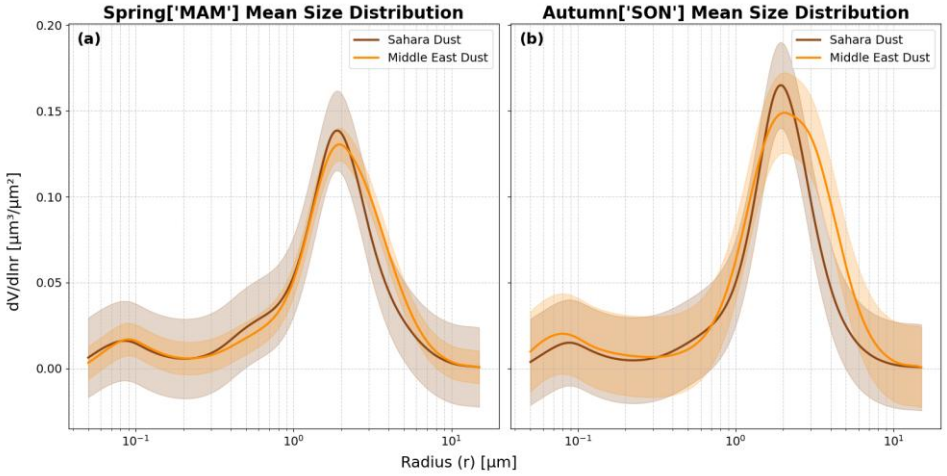

Figure S1: Mean volume size distributions for MAM (a) and SON (b) dust events, comparing Saharan (SH; brown) and Middle Eastern (ME; orange) dust layers during the study period 2015–2022. The shaded area denotes ±1 standard deviation.

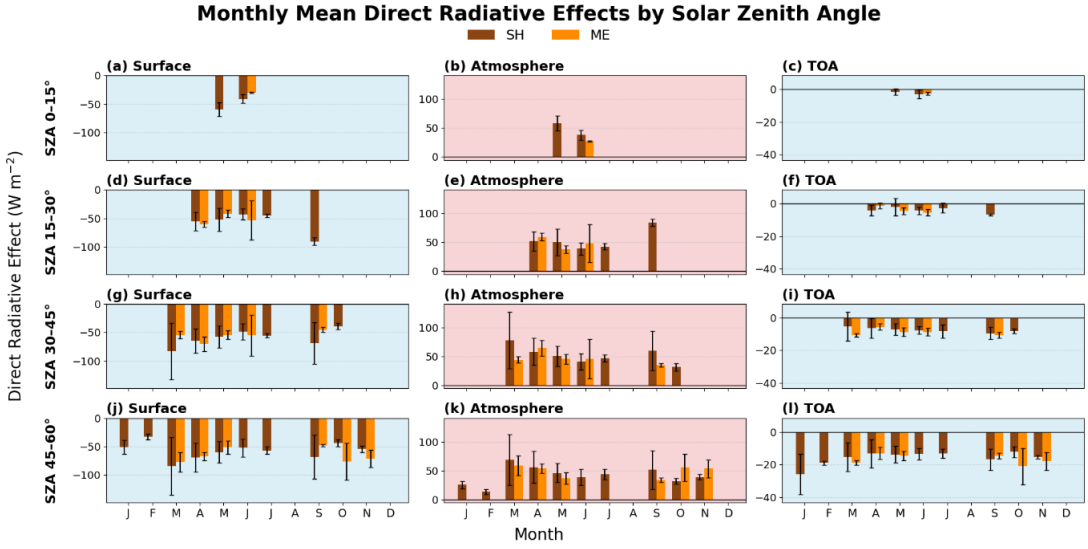

Figure S2: Monthly mean shortwave direct radiative effects (DRE; W m⁻²) over AMX during 2015–2022 under clear-sky dust conditions, classified into four solar zenith angle (SZA) intervals: 0–15°, 15–30°, 30–45°, and 45–60°. Results are shown for the surface (left column), atmosphere (middle column), and top of the atmosphere (TOA; right column). Saharan dust events are shown in brown and Middle Eastern dust events in orange. Bars represent monthly mean DRE values within each SZA interval, and error

bars denote ±1 standard deviation, indicating the variability among the instantaneous observations included in each monthly mean. Background shading denotes cooling effects in blue and atmospheric heating in red.

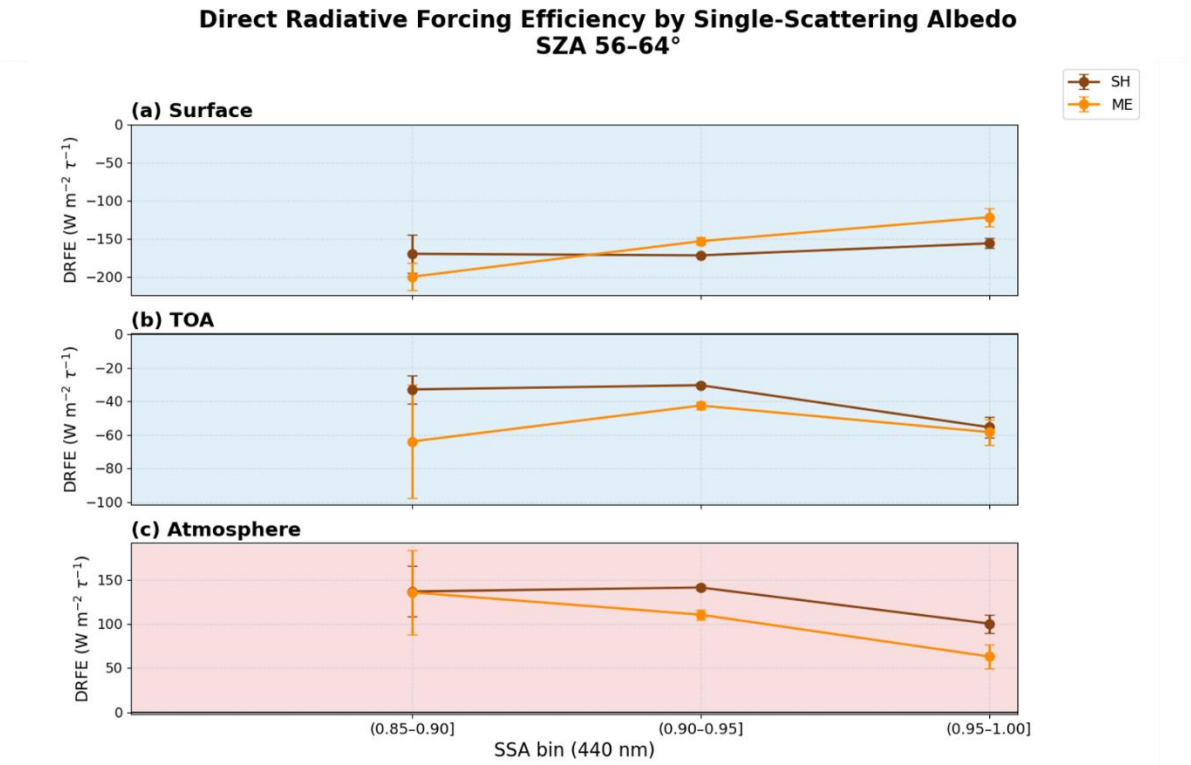

Figure S3: The DRFE (in W m⁻² τ⁻¹) as a function of SSA at 440 nm for (a) surface, (b) TOA, and (c) atmosphere, for Saharan (brown) and Middle Eastern (orange) dust. Symbols represent mean values within SSA bins and error bars denote ±1σ. Background colors denote cooling (blue) and warming (red) effects.

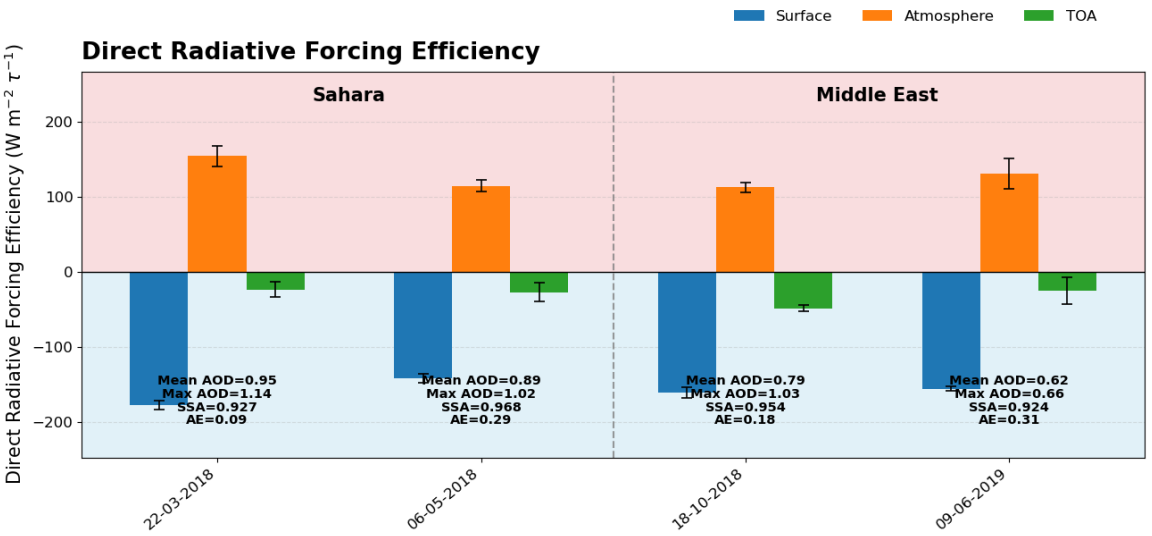

Figure S4: **DRFE at the surface, within the atmosphere, and at the TOA for the selected four dust events.**

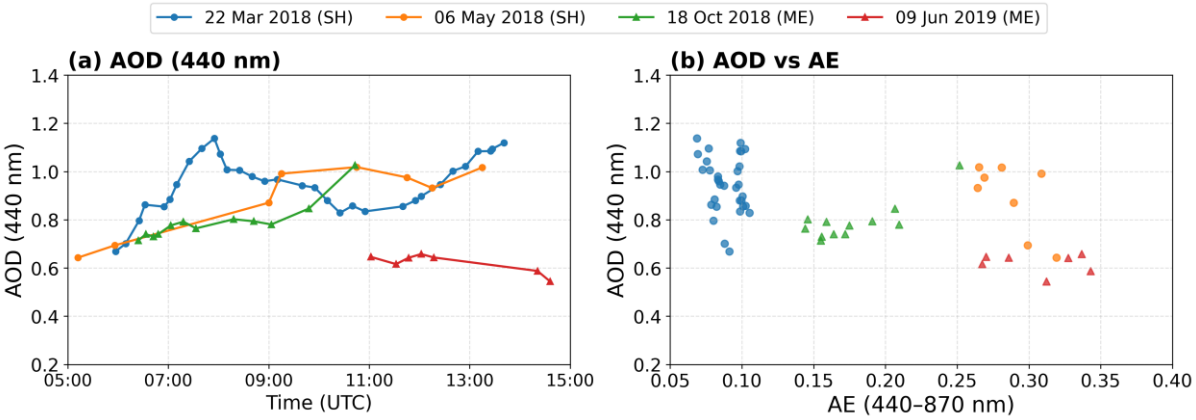

Figure S5: (a) Temporal evolution of AOD at 440 nm for four selected dust events (22 March 2018, 06 May 2018, 18 October 2018, and 09 June 2019). (b) Corresponding relationship between AOD_{440} and $AE_{440-870}$ for the same events. 22 March 2018 (Saharan; blue circles), 06 May 2018 (Saharan; orange circles), 18 October 2018 (Middle Eastern; green triangles), and 09 June 2019 (Middle Eastern; red triangles).

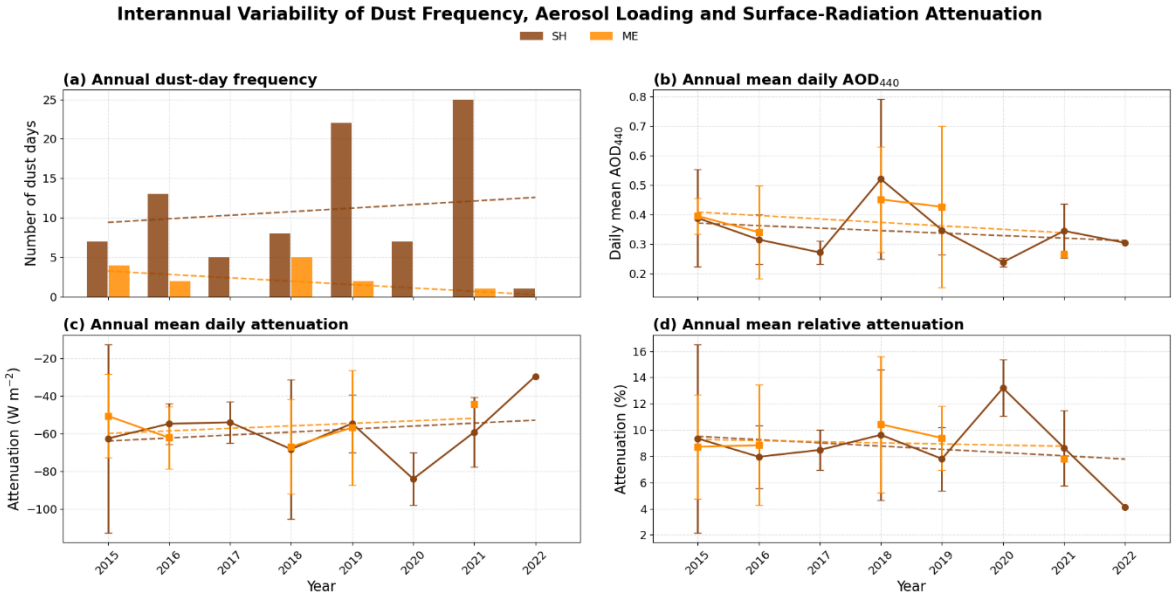

Figure S6: Interannual variability of (a) annual dust-day frequency, (b) annual mean daily AOD_{440}, (c) annual mean daily surface attenuation (DRE), and (d) annual mean relative attenuation (%) for Saharan (SH) and Middle Eastern (ME) dust over the study period (2015–2022). Error bars represent ±1 standard deviation. Dashed lines indicate linear trends.

60